Article

# Fluorinated Boronic Acid-Appended Pyridinium Salts and 19F NMR Spectroscopy for Diol Sensing

Jörg Axthelm, Sven H.C. Askes, Martin Elstner, Upendar Reddy Gandra, Helmar Görls, Peter Bellstedt, and Alexander Schiller

*J. Am. Chem. Soc.*, **Just Accepted Manuscript** • DOI: 10.1021/jacs.7b01167 • Publication Date (Web): 18 Jul 2017

# Fluorinated Boronic Acid-Appended Pyridinium Salts and $^{19}$F NMR Spectroscopy for Diol Sensing

Jörg Axthelm,[†] Sven H. C. Askes,[†] Martin Elstner,[†] Upendar Reddy G.,[†] Helmar Görls,[†] Peter Bellstedt,[†] Alexander Schiller[†]*

[†]Institute for Inorganic and Analytical Chemistry (IAAC), Friedrich Schiller University Jena, Humboldtstr. 8, D-07743 Jena, Germany

**ABSTRACT:** The identification and discrimination of diols is of fundamental importance in medical diagnostics, such as measuring the contents of glucose in the urine of diabetes patients. Diol sensors are often based on fluorophore-appended boronic acids, but these severely lack discrimination power and their response is one-dimensional. As an alternative strategy, we present the use of fluorinated boronic acid-appended pyridinium salts in combination with $^{19}$F NMR spectroscopy. A pool of 59 (bio)analytes was screened, containing monosaccharides, phosphorylated and *N*-acetylated sugars, polyols, carboxylic acids, nucleotides and amines. The majority of analytes could be clearly detected and discriminated. In addition, glucose and fructose could be distinguished up to 1:9 molar ratio in mixtures. Crucially, the receptors feature high sensitivity and selectivity, are water soluble, and their $^{19}$F-NMR analyte fingerprint is pH-robust, thereby making them particularly well-suited for medical application. Finally, to demonstrate this applicability, glucose could be detected in synthetic urine samples down to 1 mM using merely a 188 MHz NMR spectrometer.

## Introduction

The identification and discrimination of diols is of fundamental importance in medical diagnostics. For instance, the selective detection of glucose in urine is of high interest for diagnosing *Diabetes mellitus*,[1, 6, 12] whereas the detection of catecholamines, such as dopamine or epinephrine, may be used for the detection of Alzheimer's disease, neuroblastoma, and pheochromocytoma.[20, 27, 34] As a consequence, numerous sensing approaches have been developed to detect these important bioanalytes. To exploit the strong affinity of boron for diols under aqueous conditions, most detection strategies featured boronic acid-labeled receptors connected directly to a chromophore with a luminescent or colorimetric response.[8-9, 11, 15, 19, 25, 31] Although, fluorescence-based receptors demonstrate high sensitivity for diols even in the nano-molar range, they lack a characteristic analyte response because the fluorescence emission is only modulated in one dimension, i.e. more or less signal intensity. To accomplish true applicability of boronic acid receptors in medical diagnostics, sensors have to respond directly and specifically to the structural character and concentration of the analyte, even in a complex matrix with potentially interfering substrates.

We propose that this issue can be addressed by using fluorinated boronic acids as sensitive and selective probes to produce characteristic $^{19}$F Nuclear Magnetic Resonance (NMR) fingerprints.[5] $^{19}$F NMR spectroscopy benefits from 100% natural abundance of the $^{19}$F-nucleus, high sensitivity towards electronic environmental changes, a high gyromagnetic ratio, the broad chemical shift range which prevents signal overlap and usually absent background signals. Remarkable results were achieved by Swager *et al.*, who used $^{19}$F probes on tungsten calixarene complexes for the identification of neutral organic compounds,[39-40] chiral amines,[41] anions,[13] and bioactive molecules.[38] The new field of boronic acid-containing receptors with $^{19}$F probes for sensing diol-containing analytes via $^{19}$F NMR has attracted considerable interest. In 1994, the group of Gabel investigated biologically relevant diols with 4-fluorophenyl boronic acid.[21] Surprisingly, only few approaches have been published with fluorinated phenylboronic acids (Figure 1). The group of James used a fluorinated formylphenylboronic acid and a chiral auxiliary amine for the determination of the enantiopurity of diols via $^{19}$F NMR.[37] Moreover, related systems using $^{1}$H, $^{11}$B, $^{13}$C NMR have been studied.[10, 29, 32] Micouin *et al.* used commercially available fluorinated boronic acid chemosensors for monitoring boronic acid-diol interaction in aqueous solution.[16] Recently, our group published an array of fluorinated boronic acid-appended bipyridinium salts.[3] Herein, $^{19}$F NMR spectra were processed into two-dimensional QR-like barcodes. This enabled an easy approach for simple diol discrimination.

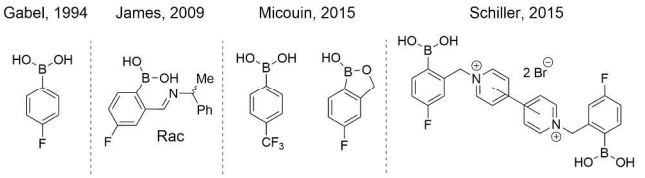


**Figure 1. Current boronic acid receptor scaffolds with attached fluorine probes used for diol sensing via $^{19}$F NMR spectroscopy with workgroups and year of publication.[3, 16, 21, 37]**

In the present study, a collection of fluorinated boronic acid-appended benzylpyridinium salts **1**-**3** (F-*o*-BBpy's) and **4** ($CF_3$-*o*-BBpy) were synthesized. These one component diol sensors contain one boronic acid function and a single fluorine/trifluoromethane moiety directly attached to the arene core (Scheme 1). Optimally performing sensor **1** was used for qualitative and quantitative $^{19}$F-NMR fingerprinting of 59 relevant bioanalytes, such as monosaccharides, phosphorylated and *N*-acetylated sugars, polyols, carboxylic acids, nucleotides and amines.

Subtle structural modifications in the probes influenced the $^{19}$F-

**Scheme 1: Reaction Scheme of Pyridinium Salts 1-6 and Molecule Structures of 1, 2 and 4[a]**

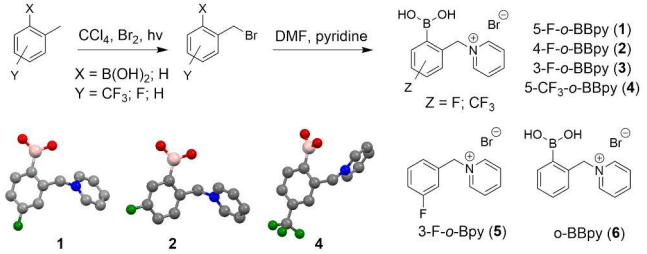


[a]Methylphenyl precursors have been photo-brominated to corresponding benzylbromides followed by *N*-alkylation with pyridine. Solvent molecules, bromide anions, and hydrogens of molecule structures are omitted for clarity; gray = C, green = F, blue = N, red = O, pink = B.

NMR response to those bioanalytes. Furthermore, several application studies were performed: discrimination of glucose and fructose in mixtures, detection of enzymatically produced D-fructose, and the detection of glucose in synthetic urine as a potential *Diabetes* test.

**Results and Discussion**

Compounds **1-6** were synthesized in two steps in high yields and excellent purities (Scheme 1). All compounds have been characterized by NMR spectroscopy, mass spectrometry, elemental analysis, UV-Vis absorption, infrared spectroscopy and potentiometric pH titration (see ESI). The molecule structures of **1**, **2** and **4** support their characterization (Scheme 1 and ESI). Crucially, all compounds exhibit high solubility (up to 77 mM for **1**) and photo stability in aqueous solution due to the high polarity of the ionic pyridinium moiety. Thus, diol screening and discrimination under physiological conditions within a broad concentration range is applicable.

Potentiometric pH titration experiments were performed to investigate the influence of the fluorine probe(s) upon the boronic acid's equilibrium between its free ($sp^2$ boron, Scheme 2) and the boronate form ($sp^3$ boron, see ESI). The non-fluorinated receptor **6** exhibits the highest p$K_a$ value (8.50). Decreased p$K_a$ values were observed for all fluorinated receptors: **2** (8.39) > **1** (8.11) > **3** (7.46) > **4** (7.14). Overall, the acidity raised with increasing content of fluorine (**6** < **1** < **4**) due to an increase in electron withdrawing (H < F < $CF_3$), while the positioning of fluorine resulted in an order in acidity of **2** < **1** < **3**. The high p$K_a$ of **2** seems to have its origin in possible fluorine-hydrogen bonding. Lowered p$K_a$ values were found for **1** in presence of D-glucose, D-fructose and D-mannitol with p$K_a$ values of 7.2, 5.4 and 6.0, respectively. It is a result of preferred $OH^-$ abstraction due to a lowered angle strain of the boronate ester (rehybridization $sp^2 \rightarrow sp^3$).[18, 22] As a matter of fact, the drop in p$K_a$ is desirable for the applicability of the sensor under physiological conditions.

As an initial $^{19}$F NMR spectroscopy experiment, 100 mM D-glucose was probed by 10 mM of compound **1** in aqueous HEPES buffer solution (100 mM, pH 7.4, 10% $D_2O$). In absence of glucose, a single $^{19}$F NMR peak was observed at $\delta_F$ –111.75 ppm for unbound **1**, whereas three additional peaks were observed in presence of D-glucose at $\delta_F$ –115.97, –117.21, and –117.26 ppm (two overlapping signals, Scheme 2). New peaks appeared baseline separated and upfield shifted.

**Scheme 2: Boronic Acid – Boronate Equilibrium and $^{19}$F Diol Fingerprinting using Fluorinated Boronic Acid-Appended Receptors under Physiological Aqueous Conditions[a]**

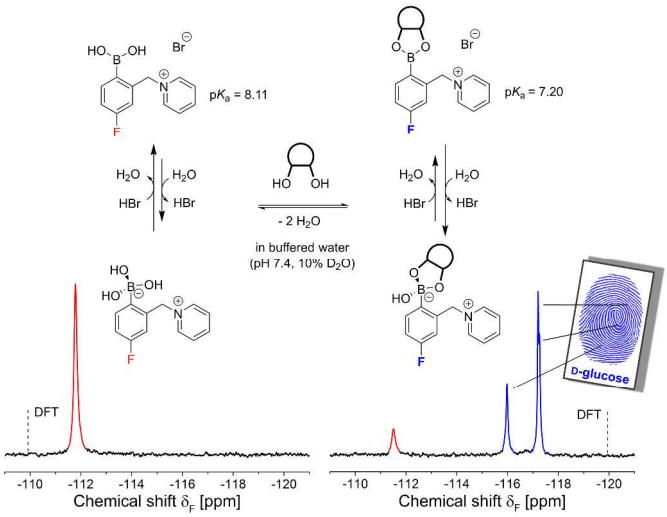


[a]The $^{19}$F probe of **1** (10 mM) recognizes the binding of D-glucose (100 mM) at the boronic acid binding site leading to highly characteristic $^{19}$F fingerprints produced by several possible binding modes (three resulting shifts). Chemical shifts have been predicted via DFT and support the trend of shift direction. Dashed lines illustrate calculated shifts (ωB97XD/6-method) of **1** ($sp^2$ / $sp^3$ of boron in the equilibrium).

Thus, indication is given that glucose binds to **1**, and that the equilibrium between free **1** and complexed **1** is slow on the NMR timescale. More importantly, this binding event had a significant effect on the electronic environment of the aromatic system and resulted in characteristic chemical shifts of the $^{19}$F probe, even over five bond lengths. The presence of three peaks reflects three distinct binding modes of glucose in the esterified sensor-glucose complex, and represents a unique $^{19}$F NMR "fingerprint". The shift to negative ppm value of the three peaks with respect to the parent compound was caused by a change in hybridization from $sp^2$ to $sp^3$, which was confirmed by predicted $^{19}$F NMR-shifts from DFT calculations (Scheme 2 and ESI). Interestingly, the chemical shift of the fingerprint did not vary within a tested pH range of 6.6 to 8.2 (ESI), demonstrating good pH robustness within the physiological pH range. This is in strong contrast to most fluorescent based boronic acids that are sensitive for changes in pH.[31] Overall, these initial results with sensor **1** established that the synthesized fluorinated boronic acids have an excellent potential as sensing and discrimination platform for diols without the need of complicated chemometric techniques.[7, 28]

Next, the $^{19}$F NMR sensing behavior was considered of the mono-fluorinated receptors 4-F-*o*-BBpy (**2**) and 3-F-*o*-BBpy (**3**), which are isomers of **1**. We were interested in how esterification affected their chemical shifts with respect to the direction, complexity and shift change. Our results showed, that the shift is strongly dependent on the position of the fluorine atom at the arene moiety. In detail, $^{19}$F signals of the pure receptors are located at $\delta_F$ –111.75 (**1**), –113.74 (**2**) and –104.84/–112.48 ppm (**3**) with fluorine in *para, meta* and *ortho* position to

boron, respectively (Figure 2a). Although only one single signal was expected for all three receptors alone, **3** is the only compound which shows a minor peak ($\delta_F$ –112.48 ppm) beside the strongly

downfield shifted main peak ($\delta_F$ –104.84 ppm). Addition of diols, such as D-glucose, D-fructose or catechol, lead to strongly upfield shifted ($\Delta\delta_F$ up to 5 ppm) $^{19}$F signals for **1**.

Receptor **3** shifted downfield ($\Delta\delta_F$ up to –2 ppm) whereas **2** showed minor upfield shifted ($\Delta\delta_F$ up to 0.6 ppm) fluorine signals. This trend supports the enhanced ability of *para*- and *ortho*-positioned fluorine probes, compared to the *meta* position, to strongly respond to changes of boron rehybridization upon diol binding via the conjugated system. The reversed direction in shifting of the *ortho* isomer **3** could be explained by the fluorine's proximity directly to the boron binding site associated with B-O-H--F- hydrogen bonding.[14, 23] Overall, the number of newly appearing receptor-diol signals is identical for all three isomers. This verifies that each $^{19}$F probe (*para*-, *meta*- and *ortho*-) recognizes the same number of formed receptor-analyte complexes. $^{19}$F NMR spectra of the monofluorinated receptors and in presence of D-glucose (b), D-fructose (c), and catechol (d) are shown in Figure 2. Going beyond, **1**-**3** can be used as an array-like sensor ensemble with a significantly enhanced diol discrimination power as we have recently reported using a set of different set of fluorinated boronic acid probes.[3]

Overall, receptor **1** was found to be the best performing diol receptor with receptor-analyte spectra of excellent signal-to-noise ratio (S/N), baseline-separated signal shifting and strong photo stability (ESI). To exclude $^{19}$F's response to other property changes than esterification the negative control 3-F-Bpy (**5**) was introduced. In detail, the $^{19}$F NMR spectrum of the non-boronic acid compound **5** (Figure S56) shows no new $^{19}$F NMR signals beside the original peak at $\delta_F$ –112.46 ppm in presence of catechol (b) or D-fructose (c). Furthermore, the signals of **5** are very sharp without distinct line-broadening from a possible

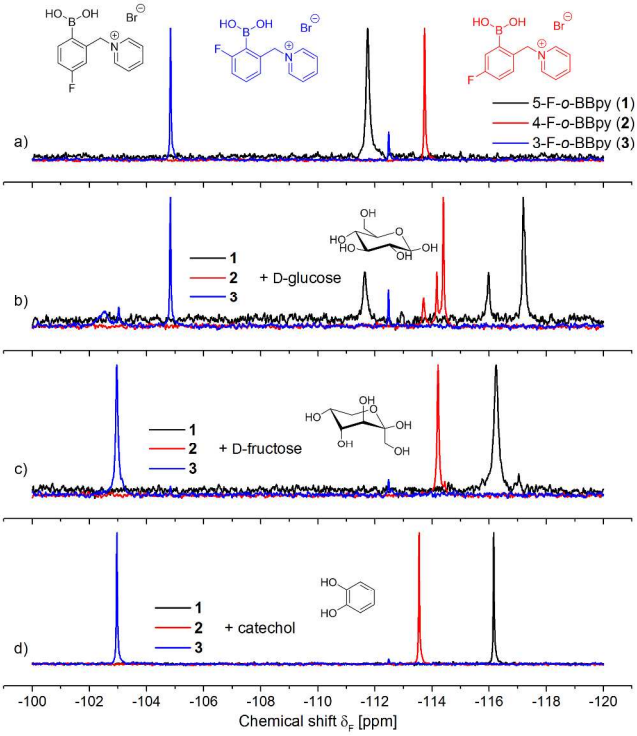


**Figure 2. Influence of the fluorine position on the $^{19}$F NMR sensing behavior of the receptors 1-3 (4 mM) and in presence of selected diols (40 mM, HEPES 100 mM, pH 7.4, 10% $D_2O$, 188 MHz, 256 scans).**

boronic acid / boronate equilibrium seen in Scheme 2. Thus, fluorine exclusively responds to diols bound at the boronic acid moiety.

Receptor 5-$CF_3$-*o*-BBpy (**4**) with a trifluoromethyl group was primarily introduced to increase the sensitivity in $^{19}$F NMR. A higher fluorine content should increase the S/N. To our delight the S/N of **4** was improved compared with **1** (~ten times, 10 mM, 188 MHz, 256 scans). However, no significant shifts in $^{19}$F NMR of **4** upon esterification with catechol and D-fructose (Figure S56c, d) could be recorded. Only a minor downfield shift of the unbound receptor at $\delta_F$ –62.66 to –62.43 ppm could be observed in the case of D-glucose (Figure S57). Thus, unfortunately compound **4** provided only very poor sensing potential due to interrupted conjugation between the boronic acid and the fluorines in the $CF_3$ moiety and the lack of characteristic $^{19}$F fingerprints. These results signify that connecting the fluorine directly to the arene boronic acid is a crucial requirement for detecting diol binding events at boron. As a result, only receptors **1**-**3** fulfill this requirement with special preference of **1**.

### Qualitative Screening of Bioanalytes using Sensor 1

Consequently, compound **1** was selected as best performing sensor and used to qualitatively screen a wide variety of analyte classes to check (i) crucial structural features of target analytes for binding, (ii) the discrimination power of the system, and (iii) to investigate $^{19}$F patterns and their correlation of structurally related target molecules. The main focus was laid on monosaccharides (aldoses and ketoses), glyceraldehyde, dihydroxyacetone, hexoses (e.g. fructose, glucose, and galactose), and phosphorylated or *N*-acetylated sugars. The pool of 59 tested analytes also included disaccharides, carboxylic

acids, simple alcohols, polyols, catechols, amines, nucleotides and one nucleoside. We wanted to understand which moieties of the analytes are crucial for successful binding. Meanwhile these experiments generated a large $^{19}$F NMR spectroscopic database of bioanalytes for discrimination purposes. A selection of the screened analyte collection with **1**, their structures and resulting $^{19}$F spectra are shown in Figure 3 (for more analytes and details see ESI). $^{19}$F NMR sensing experiments were performed in aqueous HEPES buffer solution (100 mM, pH 7.4, 10% $D_2O$, 188 MHz, 256 scans) and a receptor concentration of 10 mM whereas the analyte concentration was set to a ten-fold excess to achieve possible receptor saturation. The results are categorized according to analyte classes.

In the following, we discuss selected $^{19}$F spectra from Figure 3. Starting with blank receptor **1**, the spectrum shows the known single signal (Figure 2). In presence of D-fructose (Figure 3b), one main signal at $\delta_F$ –116.23 and a minor signal at $\delta_F$ –117.04 ppm can be found with a complete loss of the unbound signal of **1** which is completely different to the discussed fingerprint of the aldohexose D-glucose (c). This observation clearly allows the discrimination of both isomeric monosaccharides. As expected, the enantiomers with L-configuration, i.e. L-fructose (b) and L-glucose (c), produce the same spectra and allow no discrimination. With the loss of one accessible OH group in D-fructose-6-phosphate (b) compared to D-fructose, the spectrum signals are reduced to one sharp peak at $\delta_F$ –117.17 ppm. In case of D-glucose-6-phosphate (c), the spectrum was reduced to two signals at $\delta_F$ –116.53 and –117.12 ppm versus the three original signals of D-glucose. No new shifts resulted with D-glucose-1-phosphate (c), probably because of disabled isomerization possibility. Further, the three aldohexoses D-galactose, D-talose and D-mannose are represented in Figure 3e. These diastereomers can be clearly distinguished with one $^{19}$F signal at $\delta_F$ –116.07 ppm (D-galactose) and two signals at $\delta_F$ –117.00/–117.18 (D-talose) and $\delta_F$ –117.70/–117.34 ppm (D-mannose). The latter which is an epimer (inverse configuration at C-2) of D-glucose can be clearly distinguished. The same observation was found in the group of pentoaldoses D-ribose, -xylose and -lyxose (Figure 3f) which again shows the discrimination power of the system even by minor differences in the absolute configuration in one or more stereocenters. Strong affinity could be observed for diagnostic marker D/L-lactic acid (g) with a strong signal at $\delta_F$ –116.04 ppm and *N*-acetylneuraminic acid ($\delta_F$ –115.72 ppm). D-mannitol, D-sorbitol and D-dulcitol (h), which can be seen as open-ring polyols, show strong affinity to **1**. They produce one broad peak at $\delta_F$ –116.19, –115.95 and –116.17 ppm, respectively. The group of disaccharides D-maltose, D-cellobiose, and sucrose (i), result in weak diol binding at $\delta_F$ –117.01 and –117.20 ppm, respectively. Sucrose as a non-reducing sugar did not bind. In the case of the nucleotides (j), only adenosine monophosphate (AMP) produced one sharp high affinity shift at $\delta_F$ –116.99 ppm compared to ADP and ATP. However, adenosine shows a very similar spectrum compared to AMP with a fluorine signal at $\delta_F$ –116.96 ppm. Presumably, a higher grade of phosphorous residues is in competition with the OH groups of the adenosine backbone.[21] Within the group of small aliphatic alcohols containing one, two or three OH groups and amines, interestingly only 3-aminopropanol results in a strong interaction at $\delta_F$ –117.72 ppm (see ESI). Strong preference of **1** to catechol, dopamine and salicylhydroxamic acid with one single shift each was found which allows discrimination of these analytes (Figure 3k). Further spectra of receptor **1** in presence of other analytes can be found in the supporting information.

**How do Diols bind to Boronic Acid Sensor 1?**

The multitude of screened receptor-analyte complexes and their corresponding $^{19}$F NMR spectra (see Figure 2, 3, and ESI) showed primarily positive interaction in presence of reducing sugars and well preorganized diols. We also wanted to get a qualitative insight into possible diol binding modes of receptor **1** under aqueous conditions. For this purpose, we compared the recorded $^{19}$F spectra of **1** and selected analytes with theoretically possible binding modes given by the structural character of the diol. The best example is catechol with the strongest affinity. It exhibits two (syn)-1,2-OH groups in plane which are accessible to form exclusively a five-membered boronic acid-catechol ester (low p$K_a$ and strong $K_b$ values, see ESI). This is nicely represented by **1-3** which produce only a single and sharp signal in their $^{19}$F NMR spectra (Figure 2d). Catechol does not allow other isomers in solution. This observation strongly indicates that each fluorine of the receptors **1-3** reports this single receptor-catechol complex, respectively.

In contrast, monosaccharides display a complex equilibrium in water.[4] Therefore, a set of diol model analytes (cis/trans-1,3-cyclopentanediol, cis-1,2-cyclopentanediol, trans-1,2-cyclopentanediol, cis/trans-1,3-cyclohexanediol, cis-1,2-cyclohexanediol and trans-1,2-cyclohexanediol as cyclic analogues was screened to investigate favored binding of **1** to possible isomers (tautomers), such as the open-ring, α-/β-pyranose, and the α-/β-furanose forms of e.g. D-fructose. Obviously, moderate binding to only cis-1,2-cyclopentanediol could be found with one broad new appearing $^{19}$F shift at $\delta_F$ –114.69 ppm beside unbound **1**. Cis-1,2-cyclopentanediol can be seen as a furanose analogue. This result confirms the special preference of the bo-

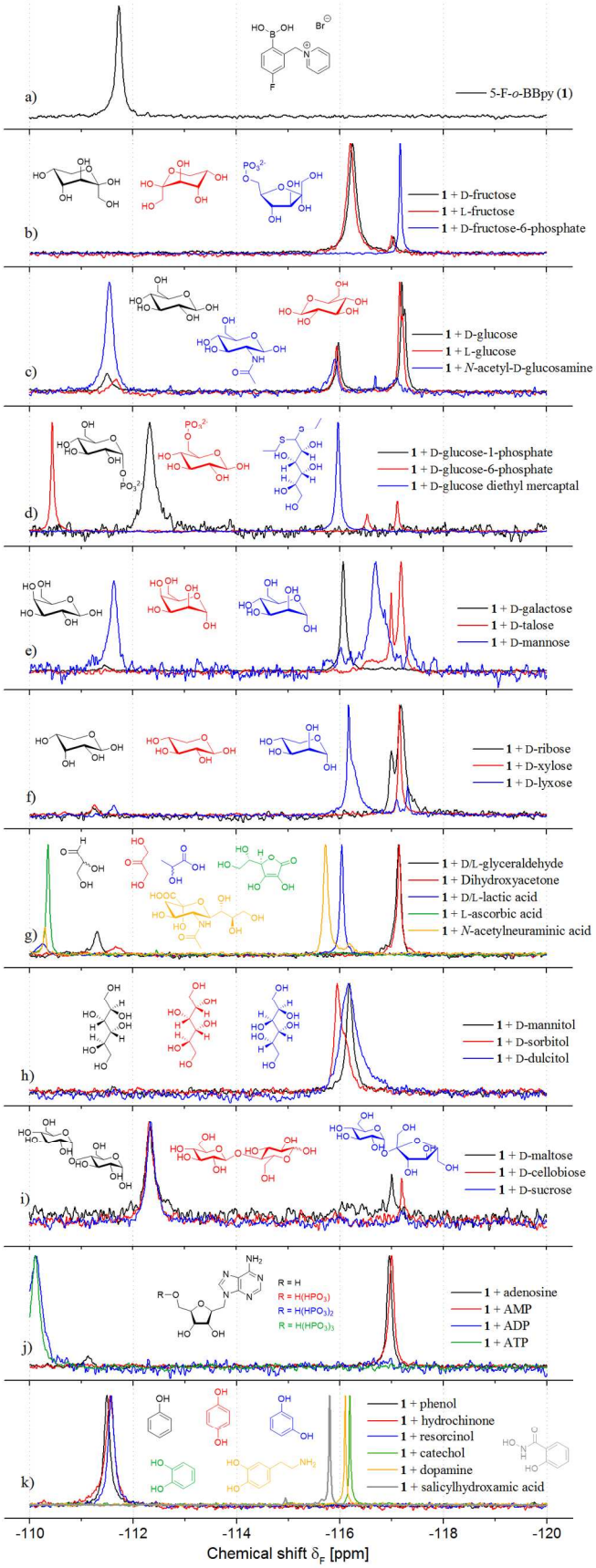


**Figure 3. Collection of discriminative $^{19}$F NMR spectra of 1 (10 mM) and diol-containing analytes (100 mM) measured in aqueous HEPES buffer solution (100 mM, pH 7.4, 10% $D_2O$, 188 MHz, 256 scans).**

ronic acid moiety to form five-membered cyclic esters with the 1,2-synperiplanar OH groups under aqueous conditions. Figure S58c represents the spectra of D-sorbitol and D-mannitol (open-ring analogues of hexoses). Both diols show very strong affinities to **1**. The shifts are in the same range as the main shift of D-fructose and the medium shift of D-glucose (Figure S58e). The exclusive binding to cis-1,2-cyclopentanediol and the strong affinities to the open ring analogues let us assume, that, under aqueous conditions, esterification of **1** with monosaccharides mainly takes place over the open ring and the α-/β-furanose form. This hypothesis can be further supported by binding constants (Table 1 and ESI) of D-sorbitol and D-mannitol which are similar to e.g. D-fructose which is known to have a high content of β-furanose with suitable synperiplanar OH groups and strong affinity to sensor **1**.[36] Another hint is the binding behavior of **1** to phosphorylated sugars. No binding to D-glucose-1-phosphate could be observed although four remaining OH groups of the α-pyranose isomer are accessible for esterification and the lack of possible open ring and furanose forms due to the blocked anomeric position (Figure 3d). In addition, D-fructose-6-phosphate and D-ribose-5-phosphate show strong affinity although no pyranose tautomers are existent beside the open-ring and furanose forms (Figure S58d). No affinity was found with the disaccharide sucrose which is a non-reducing sugar. Very weak binding to the reducing disaccharides D-maltose and -cellobiose has been recorded (Figure 3i). Nevertheless, it has to be noted that our hypothesis is in contrast to the composition of monosaccharides in solution found in literature.[4, 26] For example, a content of the β-pyranose (68%), β-furanose (22%), furanose (6%), α-pyranose (3%) and open ring form (1%) of D-fructose in $D_2O$ could be obtained via $^1$H NMR experiments.[2, 4] Thus, boron is theoretically expected to bind mainly to the β-pyranose and the α-furanose form with negligible affinity to the remaining isomers. Thus, a change of the monosaccharide tautomeric composition in presence of a boronic acid receptor, which obviously prefers the affinity to the open-ring or furanose form of suitable diol, cannot be excluded.

In order to gain insight into which diols have a high affinity for **1**, receptor-analyte binding constants of **1** with a selection of diols were determined with $^{19}$F NMR titration experiments. In detail, receptor **1** (10 mM) was titrated with appropriate diols (0 – 100 mM) until saturation. At each analyte concentration, the characteristic receptor-complex signals vary only in their relative intensity (e.g. D-mannitol, Figure S64). Thus, the absolute concentration values of unbound receptor, receptor-analyte complex(es) and resulting free analyte were quantified by signal integration. Apparent binding constants ($K_b$) were calculated using a 1:1 binding model (Table 1 and ESI).[33]

The limit of detection (LOD) and of quantification (LOQ), which specifies the $^{19}$F NMR method's sensitivity and validity under given experimental conditions (188 MHz, 256 scans), was also determined (ESI). Values were found to be in the lower millimolar range for the monosaccharides, e.g. D-fructose and D-glucose (LOD << 1 mM both, LOQ ≤ 1 and << 1 mM respectively) and in the upper micromolar range for catechol (LOD ≤ 100 µM, LOQ ≤ 400 µM) with one sharp signal.

**Diol Sensing in potential Application Scenarios**

After having determined the performance for single analyte sensing, we were interested in testing the sensor in three po-

ten- tial application scenarios with mixtures of analytes. To this end, we first investigated how sensor **1** could distinguish between D-fructose and D-glucose in binary mixtures. Receptor **1** (10 mM)

**Table 1. Apparent Binding Constants $K_b$ [$M^{-1}$] of selected Diols determined via $^{19}F$ NMR spectroscopy at pH 7.4/ 24°C.**

| Catechol | D-fructose | D-glucose | D-glucose-6-phosphate |
|---|---|---|---|
| 3980±2370 | 1620±186 | 132±33 | 144±49 |
| **D-galactose** | **D-mannitol** | **D-sorbitol** | ***N*-acetylneuraminic acid** |
| 152±5 | 807±127 | 951±93 | 123±6 |

[a]Binding constant with catechol was too high to be accurately determined, D-glucose-6-phosphate has to be treated with caution due to possible competitive receptor-phosphate interaction.

was used in a mixture of the sugars (10 mM total saccharide concentration); the mole fraction *f* of fructose was varied from 0 to 1 and for each fraction the $^{19}F$ NMR spectrum was recorded (Figure 4). Due to the highly characteristic shifts and minor signal overlap, D-glucose could be positively identified besides D-fructose up to a nine-fold excess of the latter (1 vs. 9 mM), even though it was previously found that D-fructose has a twelve-fold higher affinity for **1** compared to D-glucose (1620 vs. 132 $M^{-1}$). Vice versa, D-fructose could be at minimum positively identified at $f_{fruc}$ = 0.1 (see ESI). According to this, our approach with highly sensitive and selective fluorine probe has a considerable advantage when compared to fluorescent probes which are not able to identify the presented diols in a mixture due to non-selective signal modulation or interfering compounds.[18] In addition, **1** showed strong discrimination power of also ternary diol mixtures of D-glucose, lactate and dopamine (see Figure S61). As a consequence, our approach is a robust method and can easily be used for the identification and discrimination of diol mixtures as long as high affinity of desired analytes among interfering compounds and no signal overlap is given.

Next, we investigated whether we could monitor the production of D-fructose by sucrose-phosphorylase (SPO). It produces D-fructose and D-glucose-1-phosphate from sucrose and phosphate. Sensor **1** was mixed with SPO, sucrose, and $KH_2PO_4$ in HEPES buffer, and $^{19}F$ NMR spectra were recorded every 6 minutes (Figure S67). The characteristic fingerprint of **1** complexed with D-fructose could be clearly identified, while no other signals were detected. This is in complete agreement with our findings that both sucrose and D-glucose-1-phosphate do not bind to **1**, most likely because they are conformationally

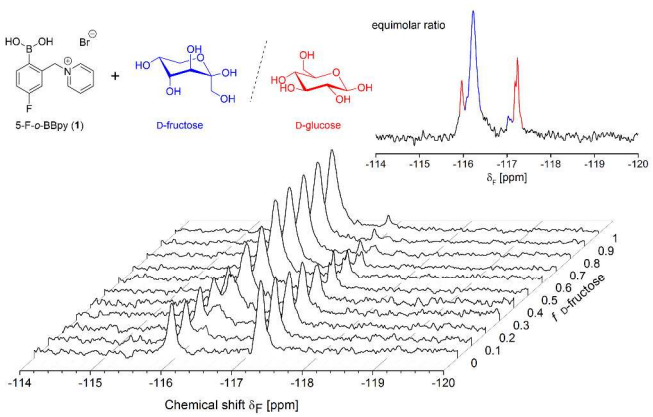


**Figure 4. $^{19}F$ Sensing of diol mixtures containing D-fructose and D-glucose via receptor 1. The fluorine spectra of 1 in presence of changing molar fraction of D-fructose illustrate the sensing potential concerning diol mixtures. D-glucose can still be identified in a mixture with D-fructose by a ratio of 1:9 respectively. Conditions: 1 (10 mM), D-fructose and D-glucose (*f* = 0-1, 0-10 mM) in HEPES buffer (100 mM, pH 7.4, 10% $D_2O$).**

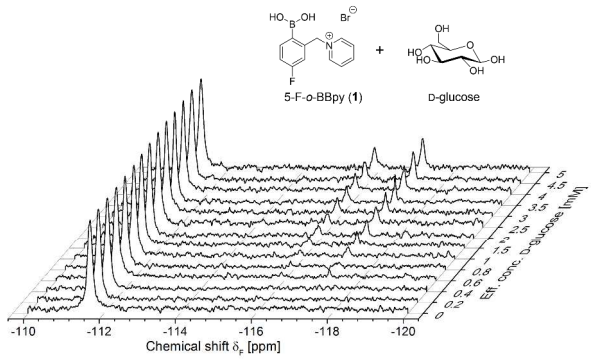


**Figure 5: Screening of D-glucose in synthetic urine assisted by receptor 1 and $^{19}F$ NMR. The spectra of 1 (10 mM) and increasing amount of D-glucose (0-5 mM) in synthetic urine (30 mM HEPES buffer, 3% $D_2O$) show the selectivity for D-glucose in a complex matrix and its applicability for a *Diabetes* Test.**

locked in the closed form (*vide supra*).[35] Thus, sensor **1** could selectively detect the production of D- fructose in a complicated mixture of salts, sugars, and enzyme.

Finally, we wanted to investigate whether sensor **1** could be used in a screening method for the diagnosis of *Diabetes mellitus*. The current diagnosis methods rely mainly on invasive blood testing, but also non-invasive techniques which determine glucose in urine samples via dip sticks are common.[12, 24] It is known that the D-glucose concentration in the urine of a healthy sober person ranges between 0 – 0.8 mM, while that of a diseased person is higher.[17, 30] To simulate a diagnostic test, a complex synthetic urine matrix was spiked with known amounts of D-glucose. The synthetic urine contained many possible interfering compounds, such as urea, KCl, creatine, and other inorganic salts. Sensor **1** was added at 10 mM to the mixtures and the $^{19}F$ NMR spectra were recorded (Figure 5). With increasing D-glucose concentration (0 – 5 mM), the characteristic shifts of the sensor-glucose complex could be observed besides the residual unbound **1**. The response of the sensor show a linear correlation of the recorded D-glucose amount versus the effective concentration of the samples. With these preliminary data, the limit of detection was ca. 1 mM, which would only indicate whether the patient is potentially diabetic or not. However, considering that we merely used a 188 MHz NMR spectrometer (256 scans, 12 min per sample), this detection limit can be easily adjusted to the sub-millimolar range for the development of an improved diagnostic procedure. Overall, it was successfully demonstrated that sensor **1** could selectively detect the presence of D-glucose in a complicated synthetic urine mixture.

## Conclusions

In conclusion, we have introduced a new set of fluorinated boronic acid-appended pyridinium salts with high water solubility, photo stability and their strong ability for diol sensing in combination with $^{19}F$ NMR spectroscopy. In comparison with

recently published similar sensors, the $^{19}$F NMR resolution and discrimination power which is assisted by unique $^{19}$F NMR diol fingerprints were significantly improved.[3] Noteworthy is that the sensors were very pH robust in the physiological range. Strong evidence was found for monosaccharides to bind to boron in the open-ring and furanose form under aqueous conditions by analyzing the recorded $^{19}$F spectra, the analytes struc-tural design and binding affinities. By varying the amount of fluorine and its relative position to the boronic acid binding site, we were able to elucidate crucial features of the receptors that are required for the application of diol sensing using $^{19}$F NMR spectroscopy. A large collection of bioanalytes was screened with the optimally performing receptor **1**. Most of the diols bind to the sensor and the resulting analyte-sensor complexes exhibited unique $^{19}$F NMR fingerprints. Thus, our approach allowed easy diol discrimination even by small structural diversity of the analytes, such as a change in only one single stereo center (epimers). Finally, to demonstrate the applicability of our results diol sensing in complicated situations, complex mixtures were tested as well. As a highlight, sensor **1** was able to detect D-glucose in synthetic urine down to 1 mM concentration, using merely a 188 MHz spectrometer.

Overall, combining $^{19}$F NMR and fluorinated boronic acids represent a robust one component system that allows selective diol identification and discrimination under physiological conditions without any interfering background signal. We expect that with continuously improving quality and cost-effectiveness of NMR spectrometers our findings are directly applicable to medical diagnostic situations. For instance, a benchtop NMR spectrometer can be used to screen urine samples of diabetes-patients in a clinical setting. We also expect that the concept can be arbitrarily widened to structurally tailor the sensor compounds for sensing specific diol subclasses and medicinal relevant catecholamines which are highly important in disease diagnosis.[27]

## ASSOCIATED CONTENT

### Supporting Information

The Supporting Information is available free of charge on the ACS Publications website at DOI: XXX.

All experimental data including synthesis, characterization of all described compounds as well as all qualitative and quantitative $^{19}$F NMR sensing experiments are located in the ESI.

## AUTHOR INFORMATION

### Corresponding Author

alexander.schiller@uni-jena.de

### Notes

The authors declare no competing financial interest.

## ACKNOWLEDGMENT

This work was supported by the German Science Foundation (DFG) via grant 1175/5-1 and the Heisenberg program SCHI 1175/4-1. We wanted to thank especially the NMR-platform (Baerbel Rambach, Gabriele Sentis and Friederike Pielenz) and the MS section (Wolfgang Poppitz, Sigrid Schoenau and Monika Heineck) of the IAAC/IOMC for the experimental realization and measuring the samples. We also like to thank Tom Desmet, Lubbert Djuikhuizen and Stefanie Graefe for the helpful discussion.

## REFERENCES

(1) American Diabetes, A. *Diabetes Care* **2017**, *40*, S11.
(2) Angyal, S. J. *Adv. Carbohydr. Chem. Biochem.* **1991**, *49*, 19.
(3) Axthelm, J.; Gorls, H.; Schubert, U. S.; Schiller, A. *J. Am. Chem. Soc.* **2015**, *137*, 15402.
(4) Barclay, T.; Ginic-Markovic, M.; Johnston, M. R.; Cooper, P.; Petrovsky, N. *Carbohydr. Res.* **2012**, *347*, 136.
(5) Chen, H.; Viel, S.; Ziarelli, F.; Peng, L. *Chem. Soc. Rev.* **2013**, *42*, 7971.
(6) Cordes, D. B.; Miller, A.; Gamsey, S.; Sharrett, Z.; Thoniyot, P.; Wessling, R.; Singaram, B. *Org. Biomol. Chem.* **2005**, *3*, 1708.
(7) Edwards, N. Y.; Sager, T. W.; McDevitt, J. T.; Anslyn, E. V. *J. Am. Chem. Soc.* **2007**, *129*, 13575.
(8) Elstner, M.; Axthelm, J.; Schiller, A. *Angew. Chem., Int. Ed.* **2014**, *53*, 7339.
(9) Elstner, M.; Weisshart, K.; Mullen, K.; Schiller, A. *J. Am. Chem. Soc.* **2012**, *134*, 8098.
(10) Fossey, J. S.; Anslyn, E. V.; Brittain, W. D. G.; Bull, S. D.; Chapin, B. M.; Le Duff, C. S.; James, T. D.; Lees, G.; Lim, S.; Lloyd, J. A. C.; Manville, C. V.; Payne, D. T.; Roper, K. A. *J. Chem. Educ.* **2017**, *94*, 79.
(11) Gamsey, S.; Miller, A.; Olmstead, M. M.; Beavers, C. M.; Hirayama, L. C.; Pradhan, S.; Wessling, R. A.; Singaram, B. *J. Am. Chem. Soc.* **2007**, *129*, 1278.
(12) Gamsey, S.; Suri, J. T.; Wessling, R. A.; Singaram, B. *Langmuir* **2006**, *22*, 9067.
(13) Gan, H.; Oliver, A. G.; Smith, B. D. *Chem. Commun. (Cambridge, U.K.)* **2013**, *49*, 5070.
(14) Gierczyk, B.; Kazmierczak, M.; Popenda, L.; Sporzynski, A.; Schroeder, G.; Jurga, S. *Magn. Reson. Chem.* **2014**, *52*, 202.
(15) Hall, D. G., Boronic Acids; Wiley-VCH: Weinheim, 2011; p 1.
(16) Iannazzo, L.; Benedetti, E.; Catala, M.; Etheve-Quelquejeu, M.; Tisne, C.; Micouin, L. *Org. Biomol. Chem.* **2015**, *13*, 8817.
(17) Ipe, D. S.; Ulett, G. C. *J. Microbiol. Methods* **2016**, *127*, 164.
(18) James, T. D.; Shinkai, S. Artificial Receptors as Chemosensors for Carbohydrates. In *Host-Guest Chemistry*; Penadés, S., Ed.; Springer Berlin Heidelberg: Berlin, Heidelberg, 2002; p 159.
(19) Jose, D. A.; Elstner, M.; Schiller, A. *Chem. Eur. J.* **2013**, *19*, 14451.
(20) Liu, L.; Li, Q.; Li, N.; Ling, J.; Liu, R.; Wang, Y.; Sun, L.; Chen, X. H.; Bi, K. *J. Sep. Sci.* **2011**, *34*, 1198.
(21) London, R. E.; Gabel, S. A. *J. Am. Chem. Soc.* **1994**, *116*, 2562.
(22) Lorand, J. P.; Edwards, J. O. *J. Org. Chem.* **1959**, *24*, 769.
(23) Madura, I. D.; Czerwinska, K.; Soldanska, D. *Cryst. Growth Des.* **2014**, *14*, 5912.
(24) Newman, J. D.; Turner, A. P. *Biosens. Bioelectron.* **2005**, *20*, 2435.
(25) Nishiyabu, R.; Kubo, Y.; James, T. D.; Fossey, J. S. *Chem. Commun. (Cambridge, U.K.)* **2011**, *47*, 1106.
(26) Polacek, R.; Stenger, J.; Kaatze, U. *J. Chem. Phys.* **2002**, *116*, 2973.
(27) Ponz de Antonio, I.; Ruiz Cantador, J.; Gonzalez Garcia, A. E.; Oliver Ruiz, J. M.; Sanchez-Recalde, A.; Lopez-Sendon, J. L. *Rev. Esp. Cardiol. (Engl Ed)* **2017**.
(28) Schiller, A.; Wessling, R. A.; Singaram, B. *Angew. Chem., Int. Ed.* **2007**, *46*, 6457.
(29) Shabbir, S. H.; Joyce, L. A.; da Cruz, G. M.; Lynch, V. M.; Sorey, S.; Anslyn, E. V. *J. Am. Chem. Soc.* **2009**, *131*, 13125.
(30) Shaykhutdinov, R. A.; MacInnis, G. D.; Dowlatabadi, R.; Weljie, A. M.; Vogel, H. J. *Metabolomics* **2009**, *5*, 307.
(31) Sun, X.; James, T. D. *Chem. Rev.* **2015**, *115*, 8001.
(32) Teichert, J. F.; Mazunin, D.; Bode, J. W. *J. Am. Chem. Soc.* **2013**, *135*, 11314.
(33) Thordarson, P. *Chem. Soc. Rev.* **2011**, *40*, 1305.
(34) Verly, I. R.; van Kuilenburg, A. B.; Abeling, N. G.; Goorden, S. M.; Fiocco, M.; Vaz, F. M.; van Noesel, M. M.; Zwaan, C. M.; Kaspers, G. L.; Merks, J. H.; Caron, H. N.; Tytgat, G. A. *Eur. J. Cancer* **2017**, *72*, 235.
(35) Vilozny, B.; Schiller, A.; Wessling, R. A.; Singaram, B. *Anal. Chim. Acta* **2009**, *649*, 246.

(36) Wu, X.; Li, Z.; Chen, X. X.; Fossey, J. S.; James, T. D.; Jiang, Y. B. *Chem. Soc. Rev.* **2013**, *42*, 8032.
(37) Yeste, S. L.; Powell, M. E.; Bull, S. D.; James, T. D. *J. Org. Chem.* **2009**, *74*, 427.
(38) Zhao, Y.; Chen, L.; Swager, T. M. *Angew. Chem., Int. Ed.* **2016**, *55*, 917.
(39) Zhao, Y.; Markopoulos, G.; Swager, T. M. *J. Am. Chem. Soc.* **2014**, *136*, 10683.
(40) Zhao, Y.; Swager, T. M. *J. Am. Chem. Soc.* **2013**, *135*, 18770.
(41) Zhao, Y.; Swager, T. M. *J. Am. Chem. Soc.* **2015**, *137*, 3221.